DNA-Dependent ATPase Activity of Bacterial XPB Helicases

Tapan Biswas, Jessica M. Pero, Caleb G. Joseph, and Oleg V. Tsodikov*

Department of Medicinal Chemistry, College of Pharmacy, University of Michigan, Ann Arbor, Michigan 48109-1065

Received December 8, 2008; Revised Manuscript Received February 4, 2009

ABSTRACT: XPB, the largest subunit of the eukaryotic transcription factor TFIIH, is essential for both initiation of transcription by RNA polymerase II and nucleotide excision repair (NER). XPB belongs to the SF2 superfamily of monomeric helicases. XPB helicase is thought to have evolved in eukaryotes; however, a gene highly homologous to human *XPB* can be found in a number of bacteria. This report is the first biochemical characterization of XPB homologues from bacteria, specifically those from *Mycobacterium tuberculosis* and *Kineococcus radiotolerans*. Similarly to eukaryotic XPB, bacterial XPB are ATP-dependent 3′ → 5′ DNA helicases. The ATPase activity of these XPB helicases is DNA-dependent, requiring a minimum of 4-nucleotide long single-stranded DNA (ssDNA). The maximum rates of ATP hydrolysis are about 10 and 50 molecules per minute by one XPB monomer on a 21-nucleotide ssDNA oligomer and on 5-kb long circular ssDNA, respectively. The ATP hydrolysis by the bacterial XPBs is coupled to their translocation along single-stranded DNA. The hydrolytic activity is strongly dependent on both the nature of a nucleotide triphosphate and that of a divalent metal. The inefficient ATP hydrolysis by bacterial XPB is consistent with nonprocessive functions of its eukaryotic homologue in locally remodeling DNA during transcription initiation and NER.

A eukaryotic 10-protein complex, TFIIH, is essential for both initiation of transcription by RNA polymerase II (Pol II) and nucleotide excision repair (NER)[1] (*1, 2*). XPB (ERCC3), the largest subunit of TFIIH, belongs to superfamily SF2 of ATP-dependent DNA or RNA helicases (*3*). *ERCC3* was initially identified as a gene correcting a DNA repair deficiency in XP-B cells from patients suffering from a severe genetic syndrome xeroderma pigmentosum (*4, 5*). Pioneering studies in yeast demonstrated that Rad25 (Ssl2), the *Saccharomyces cerevisiae* homologue of XPB, was essential for viability (*6*). Later studies pinpointed the essential roles of Rad25 in transcription (*7, 8*) and nucleotide excision repair (*2, 8*). It is established that mutations in XPB are associated with three NER and transcriptional genetic disorders in humans: xeroderma pigmentosum (XP), Cockayne syndrome (CS), and trichothiodystrophy (TTD) (*9*−*12*). The hallmarks of these syndromes are extreme sensitivity of skin and eyes to UV light and predisposition to skin and eye cancer (XP, XP/CS, TTD) and neurological and developmental abnormalities (CS, XP/CS, TTD).

Studies of TFIIH reconstituted without XPB or with ATPase-deficient mutants of XPB provided direct evidence for the requirement of XPB in ATP-dependent local 3′ → 5′ unwinding of duplex DNA at Pol II promoters or at sites containing distorting DNA lesions (*8, 13*−*15*). Refining these proposals, recent studies established that the processive helicase activity per se does not cause DNA unwinding during transcription initiation (*16*) or NER (*17*). TFIIH containing helicase-defective (but ATPase-active) mutants of XPB was shown to support dual incision of a DNA lesion by NER endonucleases (*17*). The helicase function of XPB was proposed to facilitate promoter escape of Pol II into a processive elongation mode (*16, 18*−*21*). At the same time, the ATPase activity of XPB was proven to be essential for DNA opening in transcription initiation and NER as well as for helicase functions of XPB (*16, 17*). In eukaryotes, the activity of XPB is modulated not only by its interactions with other subunits of TFIIH (*22, 23*) but also by regulatory factors of the proteasome such as SUG1 (*24*) or apoptosis pathway, e.g., p53 (*25, 26*) and p185BCR-ABL (*27*−*29*).

Detailed mechanistic and structural studies of XPB functions have been limited, in part due to the lack of a simple model system. The majority of TFIIH genes are absent in both bacteria and archaea. Thus the most significant evolutionary development of pathways that employ TFIIH appears to have occurred within the eukaryotic kingdom. Archaea contain genes with modest homology to eukaryotic *XPF*, *XPG*, *XPB*, and *XPD*. Some of these homologues have been shown to have *in vitro* activities that are generally related, but not identical, to those of their eukaryotic counterparts (*30*−*36*). Archaeal XPB homologues share 23−28% identity with human XPB and consist of only the helicase core region (Figure 1). Eukaryotic XPB proteins, in addition to the central helicase core domain, contain the N-terminal and the C-terminal domains with functions in both repair and transcription (*37*−*40*) (Figure 1). A recent study by Fan et al. revealed the structure of an XPB homologue from an archaeon *Archaeoglobus fulgidus* and demonstrated that the archaeal XPB is an active helicase *in vitro* (*33*). The extent of a functional overlap between the eukaryotic and archaeal nucleotide excision repair systems *in vivo* remains to be established.

* To whom correspondence should be addressed. Tel: (734) 936-2676. Fax: (734) 647-8430. E-mail: olegt@umich.edu.

[1] Abbreviations: NER, nucleotide excision repair; XP, xeroderma pigmentosum; nt, nucleotide; ssDNA, single-stranded DNA.

10.1021/bi8022416 CCC: $40.75
Published on Web 02/06/2009

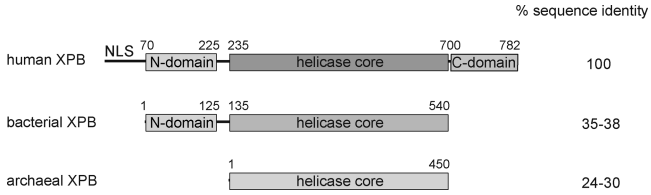

FIGURE 1: Domain organization of XPB homologues. The total sequence identity is calculated over the length of the conserved domains for a given homologue relative to the respective sequences of human XPB. The numbers at the start and the end of the domains are approximate domain boundaries.

In this work, we took advantage of the presence of genes in some bacteria that are highly homologous to the human *XPB* gene. The high degree of sequence conservation makes bacterial XPB an excellent model system for structural and functional studies. This is the first report of cloning, expression, purification, and functional *in vitro* studies of bacterial XPB.

MATERIALS AND METHODS

Cloning, Expression, and Purification of Mycobacterium tuberculosis and Kineococcus radiotolerans XPB Helicases. Genes encoding XPB homologues from *M. tuberculosis* H37Rv (mtXPB; locus tag Rv0861c; Figure S1 in Supporting Information) and *K. radiotolerans* SRS30216 (krXPB; locus tag Krad_3612; Figure S1 in Supporting Information) were PCR-amplified from genomic DNA from these bacteria. The mtXPB and krXPB genes were cloned between *Nde*I and *Xho*I and between *Nde*I and *Bam*HI restriction sites of the pET28a vector (EMD Biosciences, Madison, WI), respectively. Constructs of mtXPB bearing point mutations in ATP-binding motifs (K202E, K202R, E292A) were generated by using the QuikChange mutagenesis kit (Stratagene, La Jolla, CA). These mutations are known to inactivate other ATPases, including a yeast homologue of XPB (*41*). The sequences of all constructs were verified at the University of Michigan DNA Sequencing Core. The two full-length recombinant proteins bearing N-terminal hexahistidine tags were expressed in *Escherichia coli* BL21(DE3) and BL21(DE3)-RIL cells (Stratagene), respectively. The bacterial cultures were grown at 37 °C until an attenuance (*D*) at 600 nm of 0.3−0.4 is reached and then induced with 0.5 mM IPTG at 19 °C overnight. The cell pellets were harvested by centrifugation, resuspended in buffer A (40 mM Tris-HCl, pH 8.0, 400 mM NaCl, 10% glycerol, and 2 mM β-mercaptoethanol), and then disrupted by sonication. The proteins were purified from the clarified lysate on the Ni-IMAC columns (GE Healthcare) according to the manufacturer's instructions. The eluted proteins were concentrated and further purified on the S-200 size exclusion column (GE Healthcare), equilibrated in buffer B (40 mM Tris-HCl, pH 8.0, 600 mM NaCl, 10% glycerol, 2 mM β-mercaptoethanol, and 0.1 mM EDTA). Fractions corresponding to the monomeric helicase peak were pooled, concentrated, and used in the biochemical assays. Two mtXPB constructs lacking the N-terminal domain (proteins containing residues 124−542 and 136−542) were cloned and expressed analogously to the full-length mtXPB. These truncated proteins were completely insoluble when expressed. All three mtXPB point mutants of mt XPB (K202E, K202R, E292A) were also expressed as fully insoluble proteins. Nevertheless, identical purification protocol was followed with these expression cultures to obtain protein fractions that were used as a control for a contaminant ATPase.

Preparation of DNA Substrates for Helicase Assay. Desalted DNA oligomers from Operon Biotechnologies, Inc., A (5′-CGTGACATGCCGTGACTAGCTTTTTTTTTTT-TTTTTTTT-3′), B (5′-GCTAGTCACGGCATGTCACG-3′), C (5′-TTTTTTTTTTTTTTTTTTTTCGTGACATGCCGT-GACTAGC-3′), D (5′-TTTTTTTTTTTTTTTTTTTTGCTA-GTCACGGCATGTCACG-3′), E (5′-GCTACTCTAC-TACATCTGATCGGCTAGTCACGGCATGTCACG - 3′), F (5′-CGATCAGATGTAGTAGAGTAGC-3′), G (5′-GC-TAGTCACGGCATGTCACGGCACTGTACGGCACTG-ATCG-3′), and H (5′-CGATCAGTGCCGTACAGTGC-3′), were purified by denaturing polyacrylamide (12%) gel electrophoresis using standard protocols (*42*). To form DNA substrates using oligomers A−H, oligomers labeled with [γ-^{32}P]ATP by using T4 polynucleotide kinase (NEB) and unlabeled oligomers were mixed at 1:1.4 ratio as follows: (A + *B) 3′-overhang, (*B + C) 5′-overhang, (*A + D) splayed arm, (*A + E + F) 3′-flap, (*C + G + H) 5′-flap, where the asterisk denotes the radioactively labeled oligomer. Annealing was carried out by heating the oligonucleotide mixtures (at the final concentration of 0.5 μM) to 95 °C and then slowly cooling them to 22 °C in 2 h in a buffer containing 20 mM Tris-HCl (pH 8.0), 0.5 mM EDTA, and 0.05 M NaCl. The annealed substrates were stored at −20 °C and thawed in ice before use. The annealing was confirmed by native PAGE gel analysis. Here and throughout the text, DNA concentrations are given in terms of oligonucleotides (or annealed substrates), unless specified otherwise.

Helicase Assays. The helicase assay was performed in 10 μL of helicase buffer (25 mM Tris-HCl (pH 7.5), 50 mM NaCl, 5 mM $MgCl_2$, 1 mM ATP, and 1 mM dithiothreitol (DTT)) using 0.05 μM ^{32}P-labeled substrate and 5 μM XPB. After preincubation for 5 min at 37 °C, unlabeled competitor DNA (complement of an unlabeled strand at final concentration of 1 μM) was added to prevent reannealing of the displaced radiolabeled oligonucleotide. The unwinding reaction was carried out at 37 °C for 30 min. The reaction was stopped by adding 5× termination buffer (125 mM EDTA, 5% SDS, 12.5% glycerol, and 0.1% bromphenol blue). The reaction product was separated on a 6% native polyacrylamide (19:1) gel in 1× TAE buffer at 10 V/cm for 90 min immediately following termination and then quantified using a Typhoon phosphorimager (GE Healthcare).

DNA Substrates Used in the ATPase Experiments. For measuring ATPase activity, we used the following desalted single-stranded DNA substrates (Operon Biotechnologies, Huntsville, AL): 2-nt, 5′-GT-3′; 3-nt, 5′-GTA-3′; 4-nt, 5′-ACTC-3′; 5-nt, 5′-CACTC-3′; 6-nt, 5′-CCACTC-3′; 10-nt, 5′-CACGCCACTC-3′; 13-nt, 5′-ACTCACGCCACTC-3′; 17-nt, 5′-CACCACTCACGCCACTC-3′; 21-nt, 5′-GCCA-CACCACTCACGCCACTC-3′ and 5386-nt circular X174 virion DNA (NEB, Ipswich, MA).

ATP Hydrolysis Assays. The ATPase assays were carried out in ATPase buffer (50 mM Tris, pH 7.7, 60 mM NaCl, 1% glycerol, 5 mM $MgCl_2$ (or another divalent metal, where applicable), and 2 mM β-mercaptoethanol) at 37 °C. These concentrations were final, prepared by taking into account added NaCl, glycerol, and Tris from the protein storage

buffer (see above). Single-stranded DNA and ATP (or another ribonucleotide, where indicated) were added at required concentrations, as specified in the figures. The ATPase assays were initiated by the addition of mtXPB or krXPB proteins at the final concentration of 0.18 μM (in all ATPase assays). Each ATPase rate reported in this work was calculated by carrying out a series of absorbance measurements as a function of time in duplicate. The detection of accumulated inorganic phosphate product was based on a previously reported procedure (*43*). At given time points, 100 μL reactions were diluted 2-fold in water and quenched by the addition of 800 μL of malachite green reagent (2:1:1:2 ratio of 0.0812% (w/v) malachite green, 2.32% (w/v) polyvinyl alcohol, 5.72% (w/v) ammonium molybdate in 6 M HCl, water). After 30 s, 100 μL of 34% (w/v) sodium citrate was added and mixed. The mixture was incubated for 20−30 min at room temperature for full color development, and absorbance at 620 nm was then measured. The absorbance was stable for at least 1 h after reactions were quenched. The relationship between the absorbance and phosphate concentration was established by using KH_2PO_4 as a standard (data not shown) and used to calculate phosphate concentrations in the ATPase assays. In the above setup, this relationship was linear up to absorbance values of 1.8−2.0. We confirmed that the presence of the hexahistidine tag had no observed effect on ATPase activity (see Figure S3 in Supporting Information).

Analysis of the Steady-State Kinetics of ATP Hydrolysis. In large excess of ATP over XPB, the steady-state rate of ATP hydrolysis is a linear function of the concentration of XPB−DNA complexes (PD):

$$V^{obs} = [PD]_0 V_{PD}^{obs} \quad (1)$$

where V_{PD} is the rate of hydrolysis per one DNA-bound XPB monomer. Here, $[PD]_0$ designates the sum of concentrations of ATP-bound, ADP-bound, and unbound PD species (see the mechanism (eq 5)). For 1:1 XPB−DNA binding, the mass-action law yields the concentrations of XPB−DNA complexes ($[PD]_0$) and free XPB ($[P]_0$) (eqs 2 and 3):

$$[PD]_0 = [P^*]_{tot} - [P]_0 \quad (2)$$

$$[P]_0 = \frac{-1 + K_{DNA}^{-1}([P^*]_{tot} - [D]_{tot}) + \sqrt{(-1 + K_{DNA}^{-1}([P^*]_{tot} - [D]_{tot}))^2 + 4K_{DNA}^{-1}[P^*]_{tot}}}{2K_{DNA}^{-1}} \quad (3)$$

where $[D]_{tot}$ and $[P^*]_{tot}$ are total concentration of DNA and XPB−ATP complexes, respectively, in the reaction mixture and K_{DNA} is the equilibrium dissociation constant for ATP-associated XPB−DNA complex formation. Because we observe DNA binding indirectly, by monitoring ATP hydrolysis, we are detecting binding of DNA only to ATP-bound protein species (designated by the *). ATP is in large excess over protein, and therefore the concentration of ATP-bound protein species is related to total concentration of XPB ($[P]_{tot}$) by the hyperbolic dependence:

$$[P^*]_{tot} = [P]_{tot}\frac{[ATP]}{K_{ATP} + [ATP]} \quad (4)$$

where K_{ATP} is determined as described below. Conversely, because ATP hydrolysis is observed only in the presence of DNA, we detect ATP binding only to DNA-bound species. Because the experiments which we use to measure [DNA]-dependent ATPase rates are generally carried out at conditions $[ATP] \gg [D]_{tot} \gg [P]_{tot}$, the ability of ATP or DNA to bind free protein has no effect on the analysis. The equilibrium binding constants for mtXPB−DNA and krXPB−DNA complex formation with the single-stranded 21-mer and 10-mer were estimated from the dependence of the rate of ATP hydrolysis on DNA concentration using nonlinear regression analysis of the data according to eqs 1−3 using SigmaPlot 9.0 (Systat Software, San Jose, CA).

The observed steady-state phosphate accumulation kinetics in large excess of ATP over XPB can be described by the minimal three-step binding−hydrolysis−release mechanism (eq 5):

$$PD + ATP \overset{K_{ATP}}{\rightleftharpoons} PD{\cdot}ATP \xrightarrow{k_{cat}} PD{\cdot}ADP{\cdot}P_i \xrightarrow{k_r} PD + ADP + P_i \quad (5)$$

where K_{ATP} is the equilibrium dissociation constant for the ATP binding step, k_{cat} is the rate constant of the hydrolysis step, and k_r is the rate constant of product release. If release of phosphate (P_i) and ADP occur sequentially, then k_r is the rate constant of the slower of these two steps. If the ATP-binding step is in rapid equilibrium with respect to the subsequent hydrolytic step, then $K_m = K_{ATP}$ in the rate law for the steady-state ATP hydrolysis by one DNA-bound XPB monomer for this mechanism (also see eq 1):

$$V^{obs} = \frac{k_{cat}k_r/(k_{cat} + k_r)[ATP][PD]_0}{K_m k_r/(k_{cat} + k_r) + [ATP]} = \frac{V_{max}^{obs}[ATP]}{K_m^{obs} + [ATP]} \quad (6)$$

where

$$K_m^{obs} = K_m k_r/(k_{cat} + k_r) \quad (7)$$

and

$$V_{max}^{obs} = [PD]_0 k_{cat}k_r/(k_{cat} + k_r) \quad (8)$$

Nonlinear regression analysis of the dependence of the rate of hydrolysis on the concentration of ATP using eq 6 was performed using SigmaPlot 9.0 to obtain K_m^{obs} and V_{max}^{obs}. If the hydrolytic step is much slower than the product release and the above rapid equilibrium approximation holds, these observed parameters are equal to the intrinsic equilibrium binding constant for ATP binding (K_{ATP}) and the rate constant for ATP hydrolysis (k_{cat}), respectively. As we reported in Results, V_{max}^{obs} for 21-base and shorter oligomeric ssDNA was limited by a slow unimolecular conformational change step upon XPB binding to DNA or dissociating off a DNA end rather than the covalent bond breaking or product release steps (see Results). This rate-limiting step is likely to be implicit in k_{cat} in the simplified mechanism (eq 5). More detailed kinetic studies addressing the possible order of ATP and DNA binding to XPB and the translocation mechanism are ongoing in this laboratory.

RESULTS

A Family of Bacterial XPB Proteins. A decade ago, Poterszman et al. identified a human *XPB*-like gene in the

genome of *Mycobacterium leprae* (*44*). With many more complete genomic sequences available today, we have performed a BLAST (*45*) search for homologues of *XPB* in bacteria and archaea (see Figure S1 in Supporting Information). Genes highly homologous to *XPB* were found in a number of actinomyces, not limited to mycobacteria, and in spirochaetes, clostridia, cyanobacteria, and proteobacteria. The bacterial XPB proteins contain not only the highly conserved human XPB-like helicase core domain but also an N-terminal domain (designated N-domain in Figure 1). The N-domain in eukaryotes is responsible for binding the p52 subunit of TFIIH. Intriguingly, homologues of p52 and other TFIIH subunits are absent in bacteria. The C-terminal 60−70-residue region (designated C-domain in Figure 1) of mammalian XPB, which functions in regulation of transcription and repair and contains a nuclear localization signal (*23*), is absent in the bacterial XPB. Such a high degree of conservation of sequence and domain organization points to a close functional relationship between the human and bacterial XPB. Interestingly, Thr119 in the N-terminal domain of XPB whose mutation (to a Pro) is found in two TTD patients (*46, 47*) is universally conserved in bacterial and eukaryotic XPB. We cloned, expressed in *E. coli*, and purified to homogeneity XPB homologues from two actinomyces, *K. radiotolerans* (krXPB, with 38% amino acid residue sequence identity to human XPB) and *M. tuberculosis* (mtXPB; 36% identity), as described in Materials and Methods. The two XPB proteins behave similarly throughout purification and elute on the size-exclusion column in two forms: as large aggregates in the void volume and as a monomeric species (Figure S2 in Supporting Information). The purified krXPB and mtXPB monomers (Figure 2A) are proteolytically stable and are not in equilibrium with the aggregated state, as verified by repeating size-exclusion chromatography upon overnight incubation in the storage buffer (not shown). We also cloned and expressed truncated mtXPB (mtXPB(124−542) and mtXPB(136−542); see Materials and Methods) lacking an N-terminal domain. These deletion mutants were found exclusively in the insoluble fraction of the lysate, indicating that the N-terminal domain is required for solubility and/or structural integrity of the full-length bacterial XPB.

Bacterial XPB Proteins Are ATP-Dependent 3′ → 5′ DNA Helicases. An archaeal XPB homologue from *A. fulgidus* was demonstrated to be active in unwinding a 3′-overhang but not a 5′-overhang substrate (*33*). In order to test whether *K. radiotolerans* and *M. tuberculosis* XPB proteins are active helicases *in vitro*, we performed unwinding assays using a series of radiolabeled DNA substrates of different structures. These substrates contain either a 3′- or a 5′-single-stranded overhang or both, in addition to a duplex region (see Figure 2B,C and Materials and Methods). Both krXPB and mtXPB proteins are active DNA helicases that unwind 3′-overhang, 3′-flap, and splayed-arm DNA substrates but are incapable of unwinding 5′-overhang and 5′-flap substrates (Figure 2B,C). Therefore, these bacterial XPB homologues are 3′ → 5′ helicases. The unwinding activity of bacterial XPB was observed in the presence of ATP and was not detected in the absence of ATP or in the presence of the nonhydrolyzable ATP analogue, ATPγS, thus indicating that the helicase function of XPB requires ATP hydrolysis. The amino acid sequence, domain organization, polarity of the DNA unwinding, and ATPase activity (see below) of bacterial XPB are all very similar to the respective properties of the eukaryotic XPB. It is therefore highly likely that bacterial and eukaryotic XPB proteins are functionally homologous.

Steady-State Kinetics of ATP Hydrolysis by Bacterial XPB Helicases. ATP hydrolysis by XPB was shown to be essential for function of TFIIH in both transcription initiation and NER (*8, 16−18, 48, 49*). We investigated steady-state ATP hydrolysis by mtXPB and krXPB quantitatively by measuring the concentration of accumulated phosphate product using a colorimetric assay (*43*) (see Materials and Methods). Representative linear accumulation of inorganic phosphate as a function of time is shown in Figure 3. These reactions were carried out under conditions of a large excess of ATP and single-stranded 21-mer DNA over enzyme, indicative of steady-state turnover. The mutants of mtXPB bearing a single residue substitution in conserved Walker motifs, K202E, K202R, and E292A, were expressed as completely insoluble proteins. Despite this fact, we carried out purification with all three mutants and found no significant ATPase activity in the respective fractions (data not shown). This observation and the homogeneity of the preparations of both mtXPB and krXPB, as judged by the overloaded SDS−PAGE gel (Figure 2A, Figure S2 in Supporting Information), make the presence of a contaminating ATPase in the wild-type protein preparations highly unlikely.

The steady-state ATPase kinetics, measured for krXPB and mtXPB at different concentration of ATP as shown in Figure 4, yield an [ATP]-dependent rate of inorganic phosphate accumulation. This dependence for the 10-mer and the 21-mer single-stranded DNA is well described by a hyperbolic Michaelis−Menten function (eq 6 in Materials and Methods). If the product release is not rate-limiting and the ATP binding step is in rapid equilibrium with unimolecular steps, then K_m^{obs} is interpreted as the equilibrium constant for binding ATP to an XPB−DNA complex. V_{max}^{obs} is the product of the concentration of the total protein fraction active in hydrolysis and the rate constant (k_{cat}) of the slowest step among many unimolecular steps in the turnover, such as hydrolysis, protein and DNA conformational changes upon ATP/DNA binding or upon binding and dissociation from DNA, hydrolytic product release, and potential translocation along DNA. The observed ATPase kinetics are very similar for the two helicases, with mtXPB exhibiting somewhat higher rates of ATPase activity than krXPB with either DNA substrate. For the 21-mer, V_{max}^{obs}(mtXPB, 21-mer) = 1.5 ± 0.1 μM/min and V_{max}^{obs}(krXPB, 21-mer) = 1.13 ± 0.04 μM/min of released phosphate, which corresponds to 8.3 ± 0.6 and 6.3 ± 0.2 cycles of ATP hydrolysis per minute per monomer of mtXPB and krXPB, respectively. The apparent maximum rates of ATP hydrolysis for both mtXPB and krXPB are about 2-fold slower with the single-stranded 10-mer than the respective rates with the 21-mer: V_{max}^{obs}(mtXPB, 10-mer) = 0.72 ± 0.02 μM/min and V_{max}^{obs}(krXPB, 10-mer) = 0.46 ± 0.02 μM/min. We analyze the origin of these differences in the rates of hydrolysis for the two DNA lengths in the next section. The K_m^{obs} values for both helicases are higher with the 21-mer ssDNA (K_m^{obs}(mtXPB, 21-mer) = 1.0 ± 0.1 mM and K_m^{obs}(krXPB, 21-mer) = 0.9 ± 0.1 mM) than with the 10-mer (K_m^{obs}(mtXPB, 10-mer) = 0.58 ± 0.03 mM and K_m^{obs}(krXPB, 10-mer) = 0.26 ± 0.04 mM). The somewhat smaller K_m^{obs} values for the shorter DNA may be a conse-

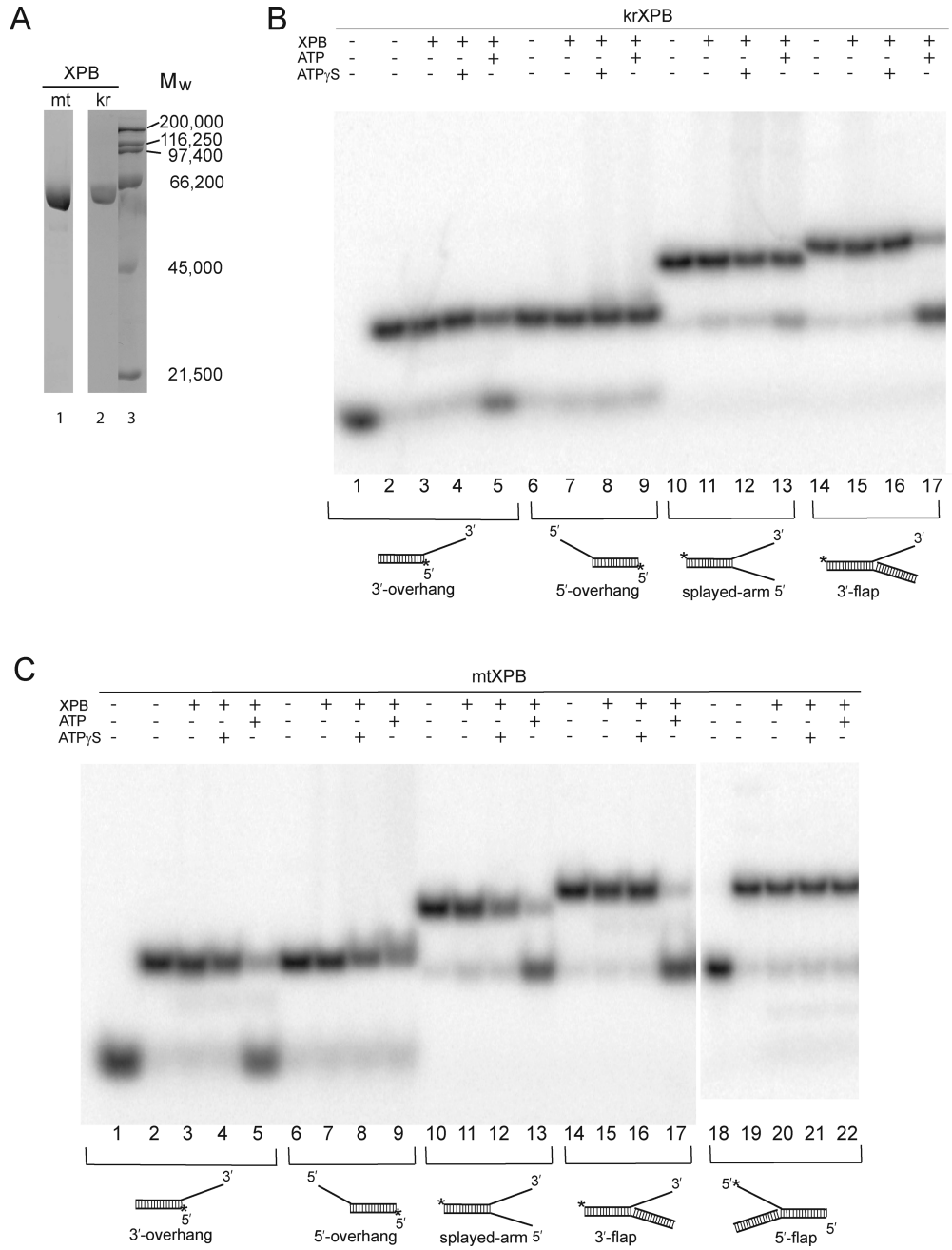

FIGURE 2: (A) A 12% Coomassie blue-stained SDS−PAGE gel showing the purified mtXPB and krXPB. (B) A phosphorimager scan of a 6% native PAGE gel demonstrating the ATP-dependent helicase activity of krXPB and (C) mtXPB on a series of DNA substrates, as indicated (see Materials and Methods). The radioactively labeled DNA end is designated by an asterisk. For a given substrate, in each lane, the top band corresponds to the substrate shown schematically below the gel and the bottom band (if present) corresponds to the single-stranded product of the unwinding reaction.

quence of the decreased electrostatic or steric repulsion between ATP and DNA bound to helicase with decreasing DNA length.

DNA Concentration Dependence of ATPase Activity of XPB Helicases. In order to investigate the origin of the observed dependence of apparent maximum rate of ATP hydrolysis (V_{max}^{obs}) on the length of the single-stranded DNA substrate, we measured the steady-state ATPase kinetics of mtXPB and krXPB as a function of DNA concentration with the 21-mer and the 10-mer substrates. The rate of phosphate accumulation increases with increasing DNA concentration and reaches a plateau (Figure 5). The ATPase rate increases as a result of the increase of the fraction of XPB bound to DNA. No significant hydrolytic activity by either XPB protein was generally observed in the absence of DNA (see also Materials and Methods). The rate dependence on DNA concentration followed a simple 1:1 binding isotherm (best-fit curves in Figure 5) from which the observed equilibrium binding constant K_{DNA} for ATP-bound XPB−ssDNA complex formation and the rate of hydrolysis by one XPB−DNA complex at [ATP] = 1 mM were obtained by a nonlinear regression analysis, as described in Materials and Methods. MtXPB binds both 21-mer and 10-mer DNA with a much higher affinity than krXPB does (K_{DNA}(mtXPB, 21-mer) < 50 nM, K_{DNA}(krXPB, 21-mer) = 10.0 ± 3.3 μM; K_{DNA}(mtXPB, 10-mer) = 22 ± 5 μM, K_{DNA}(krXPB, 10-mer) > 50.0 ± 3.3 μM). This dramatic difference in DNA affinities between mtXPB and krXPB results in the smaller fraction

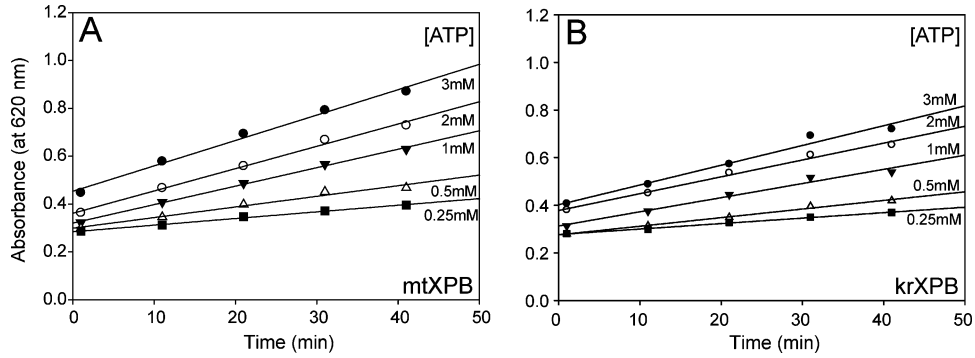

FIGURE 3: Representative time courses of accumulation of inorganic phosphate product during ATP hydrolysis using the 21-nt single-stranded DNA substrate at different ATP concentrations (as indicated) for (A) mtXPB and 10 μM DNA and (B) krXPB and 15 μM DNA, performed in both cases with 0.18 μM XPB. The linear dependence is a signature of the steady-state kinetics of ATPase activity of XPB.

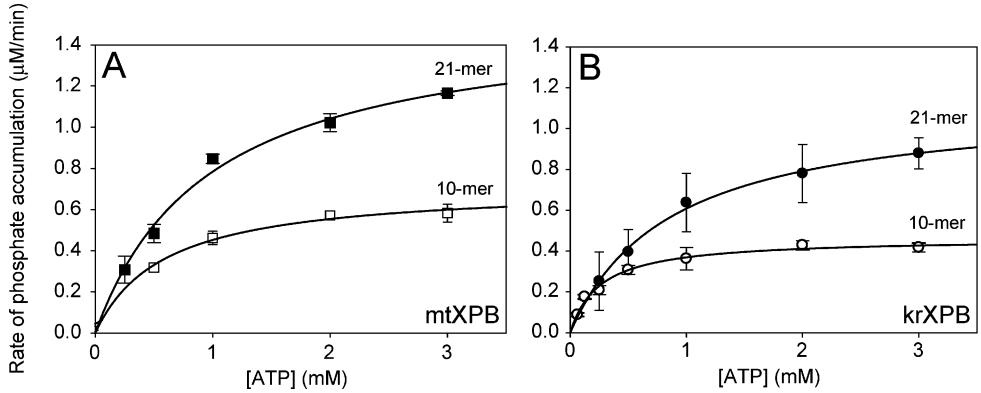

FIGURE 4: Rates of ATP hydrolysis as a function of ATP concentration. ATPase reaction with (A) mtXPB and (B) krXPB was carried out using 10 μM 21-nt (filled symbols) and 15 μM 10-nt (open symbols) single-stranded DNA substrates and 0.18 μM XPB.

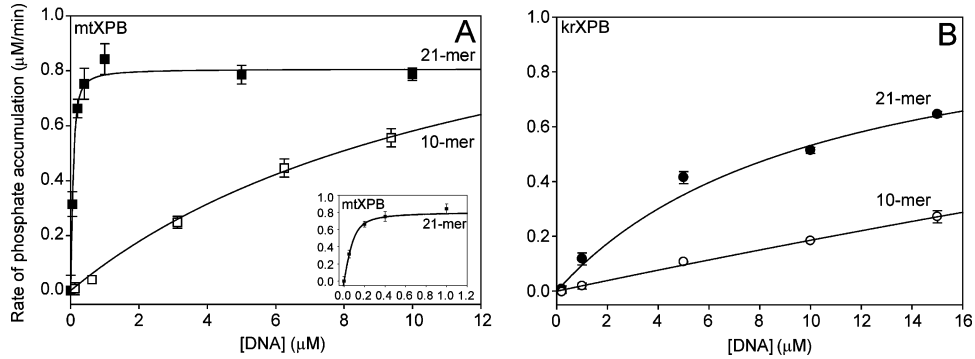

FIGURE 5: DNA substrate concentration dependence of the rate of ATP hydrolysis by bacterial XPB helicases. The reactions with the 21-nt ssDNA (filled symbols) and 10-nt ssDNA (open symbols) substrates were carried out using 1 mM ATP and 0.18 μM XPB.

of krXPB−DNA complexes than that of mtXPB−DNA complexes for the experiments shown in the previous section. In fact, for the condition of the experiments discussed in the previous section, at 10 μM 21-mer ssDNA, all mtXPB is bound to DNA, whereas at 15 μM 21-mer ssDNA, only about 60% of krXPB is bound to DNA. Both helicases bind with much stronger apparent affinities to the 21-mer than to the 10-mer ssDNA, which must result both from the larger number of available binding sites on the 21-mer than that on the 10-mer and from the additional favorable interactions with DNA flanking the site of bound XPB on the 21-mer ssDNA.

Despite these differences in DNA affinities for the two helicases and for the two DNA oligomer lengths, the maximum rates of hydrolysis by the two helicases bound to DNA turn out to be very similar. The rate of hydrolysis per one mtXPB monomer bound to 21-mer ssDNA at 1 mM ATP (equal to K_m^{obs} for ATP; see the previous section), calculated from the plateau in Figure 5, is 0.84 ± 0.07 μM/min/0.18 μM (XPB) = 4.7 ± 0.4 ATP/min. This rate, as expected, is approximately 2-fold slower than the maximum rate reported in the previous section (8.3 ± 0.6 ATP hydrolyzed/min, where all mtXPB is bound to DNA, as discussed above), as expected at this ATP concentration. Thus 8.3 ± 0.6 ATP/min is the true maximum rate of hydrolysis by one 21-mer ssDNA-bound mtXPB monomer. For krXPB, the apparent maximum rate of ATP hydrolysis measured in the previous section is only 60% of the actual maximum rate, because only 60% of krXPB is bound to the 21-mer DNA at these conditions, as shown above. Therefore, the true maximum rate of hydrolysis by one krXPB bound to 21-mer DNA calculated using this fractional occupancy

is 10.0 ± 1.5 ATP/min. The plateau rate value in Figure 5B corresponds to 5.9 ± 0.9 ATP/min hydrolyzed by one krXPB−21-mer DNA complex at 1 mM ATP (also equal to K_m^{obs} for krXPB), which is in excellent agreement with the half-maximum hydrolysis rate of 5.0 ATP/min obtained in this section. Binding of the 10-mer to mtXPB is strong enough to obtain an estimate for the rate of 7.3 ± 0.6 ATP/min at 1 mM ATP by one mtXPB−10-mer complex (from the plateau in Figure 5A). In this case, $K_m^{obs} = 0.58$ μM (see above), and therefore this rate is 63% of the actual rate, which is then 11.6 ATP/min hydrolyzed by one mtXPB−10-mer DNA. 10-mer ssDNA binding to krXPB is too weak to allow one to measure accurately the plateau rate at high DNA concentration; therefore, only a lower bound is reported. An analogous calculation yields the lower bound of the true maximum rate for one krXPB−10-mer ssDNA complex of 5.1 ATP/min. Therefore, the slower apparent maximum rate measured for krXPB with the 10-mer ssDNA than that with the 21-mer in the previous section is a consequence of a very low affinity (>50 μM) of krXPB for the 10-mer substrate.

The DNA unwinding activities of mtXPB and krXPB (described above) are in a good qualitative agreement with the respective observed ATPase kinetics. Due to a much lower K_{DNA} of mtXPB, unwinding of all DNA substrates by mtXPB was a single-turnover process and was complete within minutes (Figure 2C). In contrast, only a small population of DNA is predicted to be bound by krXPB at the conditions of the helicase assays, and therefore a large fraction of DNA remains unwound after 30 min (Figure 2B).

Dependence of ATPase Activity on the Length of Single-Stranded DNA Substrate. The above results show that the maximum rates of ATP hydrolysis by mtXPB and krXPB proteins bound to the 21-mer and to the 10-mer ssDNA are comparable for the two helicases and the two DNA oligomer lengths. This means the 10-mer is long enough to establish all interactions required for the catalysis of ATP hydrolysis. In order to determine the minimal size of ssDNA that supports ATP hydrolysis, we conducted a series of ATPase rate measurements with ssDNA substrates of different lengths, as shown in Figure 6. The shortest single-stranded oligomer supporting the ATPase activity of XPB is 4 nucleotides long; no significant ATPase activity outside of experimental uncertainty was observed with a 2-nt or a 3-nt ssDNA. Upon increase in DNA length from 4 to 6 bases, the rate increases relatively fast, indicating appearance of additional favorable interactions with DNA flanking the requisite 4 bases bound to XPB. Further relative increase of activity with DNA length beyond a (6−10)-mer is much more gradual, indicating that most important interactions with the protein have already been established and no significant increase in activity due to processivity is observed as the ssDNA length increases to 21 nt. Therefore, the minimal length of ssDNA substrate that establishes all interactions with a bound XPB for its maximal nonprocessive catalytic activity is between 6 and 10 nt. In order to test whether ATP hydrolysis involves translocation of XPB along ssDNA, we have measured the rate of ATPase activity on a long (5386-nt) circular DNA at the same total nucleotide concentration (of 210 μM) as that used in the assays with the 21-nt DNA oligomers (at this concentration all protein is bound to 21-mer or 5386-mer DNA). In this setup, the only difference between the experiment with the 21-mer and that with the 5386-mer is the presence of DNA ends in the 21-nt oligomer. The ATPase efficiency for mtXPB and krXPB is 4−5-fold higher on the long circular DNA relative to that on the 21-nt ssDNA. This result is a strong indication that XPB translocates along DNA while hydrolyzing ATP and that on the short oligomers the enzyme turnover rate is limited either by a slow unimolecular conformational change step upon XPB rebinding to DNA (after falling off an end) or by slow dissociation off a DNA end.

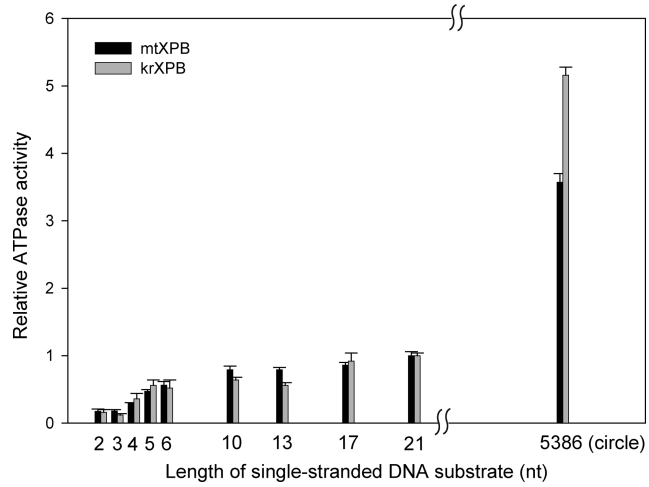

FIGURE 6: Relative ATPase activity of bacterial XPB as a function of length of single-stranded DNA. The rate of ATP hydrolysis was measured using 0.18 μM XPB with single-stranded DNA oligomers from 2-nt to 21-nt long at 10 μM (in oligomers) and with 1 mM ATP. The concentration of the circular 5386-nt single-stranded DNA was 210 μM in nucleotides, i.e., equal to that of the 21-nt substrate in order to eliminate the effect of the much larger number of binding sites for XPB on the longer DNA. The figure shows the ATPase rates relative to that measured with the 21-nt substrate

Ribonucleotide and Divalent Metal Dependence of ATPase Activity of XPB Helicases. In order to test the nucleotide specificity of XPB helicases, we compared the catalytic activity of ATP, CTP, GTP, and TTP hydrolysis by mtXPB and krXPB (Figure 7A). Both mtXPB and krXPB exhibit strong preference toward ATP. Hydrolysis of CTP and GTP was significantly (7-fold) less efficient than that of ATP; no hydrolysis of TTP was observed. This nucleotide preference is very similar for the two helicases.

MtXPB and krXPB also exhibit the same rank order of ATPase activity with respect to different divalent metal cofactors (Figure 7B). Of the ones examined, the fastest rate was observed with Mn^{2+}, similar to that with Mg^{2+}. Ca^{2+} supports hydrolysis at a lower rate than that observed with Mg^{2+} or Mn^{2+}. No significant ATPase activity was observed in Co^{2+} or Zn^{2+} with either XPB helicase.

DISCUSSION

The essential roles of eukaryotic XPB as a part of the multiprotein TFIIH complex in DNA opening during transcription initiation and nucleotide excision repair have been extensively demonstrated (*1, 2, 7, 8, 40*). However, the mechanistic and structural details of XPB function remain unclear. The ATP-dependent helicase activity of purified yeast and archaeal homologues of XPB proteins *in vitro* was shown previously (*8, 33*).

A major obstacle in elucidating the mechanism of XPB function is finding a suitable model system for carrying out

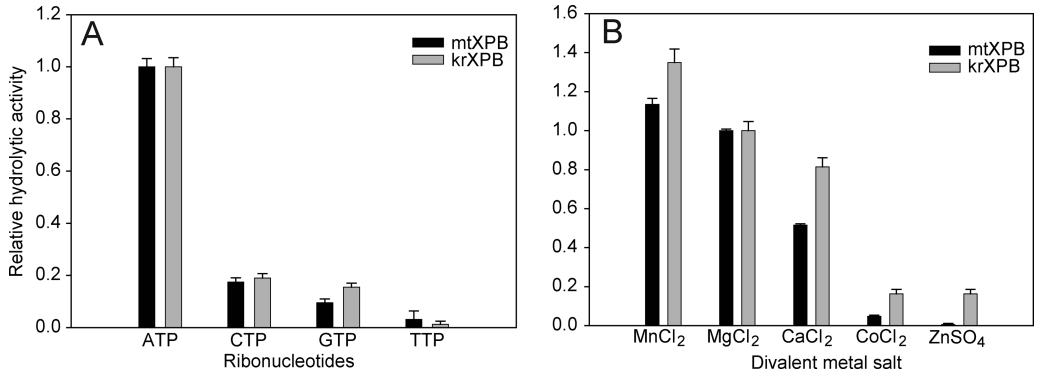

FIGURE 7: Phosphatase activity of XPB with different (A) ribonucleotides and (B) divalent metals. The rate of hydrolysis was measured using 0.18 μM XPB, 1 mM ribonucleotides (as indicated in panel A) or ATP (panel B) and 5 mM Mg^{2+} (panel A) or another divalent cation (as indicated in panel B) and 10 μM 21-mer ssDNA. The rates shown in the figure are plotted relative to those measured with (A) ATP and (B) Mg^{2+}.

quantitative biochemical and structural studies *in vitro*. Perhaps due to the modular architecture and many obligatory interactions that XPB is engaged in *in vivo*, soluble full-length human XPB protein can only be expressed in insects cells and in a very limited amount (*50*). The archaeal gene with limited homology to human *XPB* contains only the helicase core domain. A structure of XPB helicase from archaeon *A. fulgidus* was recently determined (*33*). Bacteria generally lack XPB; however, we found that a number of bacteria not limited to mycobacteria contain an XPB homologue, originally found in *M. leprae* (*44*). Given this high degree of sequence and domain conservation as well as the absence of homologues of other TFIIH subunits, it is likely that the XPB gene was acquired by bacteria through horizontal transfer from eukaryotic species (*32*). Horizontal transfer from eukaryotes to eubacteria is not well understood, although it is not uncommon. For example, a simplified version of the eukaryotic nonhomologous end joining system is present in a number of bacteria, including *M. tuberculosis* (*51*) and *K. radiotolerans* (*52*). XPB and other DNA repair genes that might have traveled from eukaryotes to bacteria may have then adapted to specific types of DNA damage or recombination. A potential role in mismatch repair is worth investigating given that both *M. tuberculosis* and *K. radiotolerans* lack classical bacterial mismatch repair genes (including *MutS*) (*52*). Perhaps coincidentally, it has been very recently shown that *MutS* gene in bacteria is a "hot spot" for horizontal gene transfer (*53*). The *in vivo* functional roles of *M. tuberculosis* XPB protein likely extend beyond DNA repair as the *XPB* gene has been predicted to be essential in *M. tuberculosis* (*54*).

Here, we demonstrated that bacterial XPB homologues are ATP-dependent DNA helicases that unwind structure-specific DNA with a defined 3′ → 5′ polarity. The sequence and domain similarities between bacterial and eukaryotic XPB proteins indicate a strong degree of functional (helicase and ATPase) homology between these proteins. We performed quantitative steady-state kinetic studies of ATPase activity of the bacterial XPB helicases using a series of single-stranded oligomeric DNA substrates of different lengths. Similarly to Rad25, the *S. cerevisiae* XPB homologue (*8*), the ATPase activity of bacterial XPB's is DNA-dependent. As ssDNA oligomers become smaller, from a 21-mer to a 10-mer, the ATPase activity gradually decreases, mainly due to the decrease in apparent DNA binding affinity (in the micromolar range) whereas kinetics of rate-limiting unimolecular steps (conformational changes and/or covalent bond breaking) remain unperturbed. Relatively weak DNA binding is common for proteins that do not bind DNA in a sequence-specific fashion and must allow for regulation of their catalytic function(s) *in vivo*. Such regulation is likely to be rendered by interactions with other DNA-binding proteins.

We showed that a 4-nt oligomer is the shortest ssDNA oligomer to support observable ATPase activity of XPB. Similarly, bacterial NER helicase UvrD requires at least a 4-nt single-stranded overhang on a duplex substrate *in vitro* (*55*). Furthermore, the ATPase activity of bacterial XPB on a long (5386-nt) circular DNA is 4−5-fold higher than that on a 21-mer. This activity increase with increasing length of ssDNA yields the maximum ATPase rate of only about 50 ATP hydrolyzed per minute per monomer of XPB. This rate is consistent with the rate of hydrolysis of 100 min^{-1} by XPB homologues from archaeon *Sulfolobus solfataricus* (*36*). This value is also comparable to 140 min^{-1} for Rad25 (*8*) and to 107 min^{-1} for another SF2 helicase, NS3, from hepatitis C virus (*56*). The relatively slow observed ATPase rate of bacterial XPB, as compared with 100-fold higher ATPase rates of processive SF1 or replicative hexameric helicases, likely signifies either that the ATPase activity of XPB is not very processive (e.g., the protein frequently pauses or dissociates from DNA) or that XPB is an intrinsically slow ATPase. Pre-steady-state kinetic studies necessary to investigate the translocation mechanism are a subject of future research in this laboratory. Generally, mechanisms of coupling of ATPase activity to function are not well understood for the very diverse SF2 superfamily of helicases. The inefficient ATP hydrolysis by bacterial XPB is consistent with limited DNA unwinding or other remodeling functions of eukaryotic XPB during isolated events of transcription initiation and excision repair.

ACKNOWLEDGMENT

We thank Dr. Lawrence Shimkets for kindly providing a *K. radiotolerans* SRS30216 culture. We are grateful to Christine Kim for assistance with the helicase assays.

SUPPORTING INFORMATION AVAILABLE

Figures showing the alignment of XPB sequences as well as controls described in the text. This material is available free of charge via the Internet at http://pubs.acs.org.

REFERENCES

1. Drapkin, R., Reardon, J. T., Ansari, A., Huang, J. C., Zawel, L., Ahn, K., Sancar, A., and Reinberg, D. (1994) Dual role of TFIIH in DNA excision repair and in transcription by RNA polymerase II. *Nature 368*, 769–772.
2. Wang, Z., Svejstrup, J. Q., Feaver, W. J., Wu, X., Kornberg, R. D., and Friedberg, E. C. (1994) Transcription factor b (TFIIH) is required during nucleotide-excision repair in yeast. *Nature 368*, 74–76.
3. Singleton, M. R., Dillingham, M. S., and Wigley, D. B. (2007) Structure and mechanism of helicases and nucleic acid translocases. *Annu. Rev. Biochem. 76*, 23–50.
4. Thompson, L. H., Carrano, A. V., Sato, K., Salazar, E. P., White, B. F., Stewart, S. A., Minkler, J. L., and Siciliano, M. J. (1987) Identification of nucleotide-excision-repair genes on human chromosomes 2 and 13 by functional complementation in hamster-human hybrids. *Somat. Cell Mol. Genet. 13*, 539–551.
5. Weeda, G., Wiegant, J., van der Ploeg, M., Geurts van Kessel, A. H., van der Eb, A. J., and Hoeijmakers, J. H. (1991) Localization of the xeroderma pigmentosum group B-correcting gene ERCC3 to human chromosome 2q21. *Genomics 10*, 1035–1040.
6. Park, E., Guzder, S. N., Koken, M. H., Jaspers-Dekker, I., Weeda, G., Hoeijmakers, J. H., Prakash, S., and Prakash, L. (1992) RAD25 (SSL2), the yeast homolog of the human xeroderma pigmentosum group B DNA repair gene, is essential for viability. *Proc. Natl. Acad. Sci. U.S.A. 89*, 11416–11420.
7. Qiu, H., Park, E., Prakash, L., and Prakash, S. (1993) The *Saccharomyces cerevisiae* DNA repair gene RAD25 is required for transcription by RNA polymerase II. *Genes Dev. 7*, 2161–2171.
8. Guzder, S. N., Sung, P., Bailly, V., Prakash, L., and Prakash, S. (1994) RAD25 is a DNA helicase required for DNA repair and RNA polymerase II transcription. *Nature 369*, 578–581.
9. Dianov, G. L., Houle, J. F., Iyer, N., Bohr, V. A., and Friedberg, E. C. (1997) Reduced RNA polymerase II transcription in extracts of cockayne syndrome and xeroderma pigmentosum/Cockayne syndrome cells. *Nucleic Acids Res. 25*, 3636–3642.
10. Tu, Y., Bates, S., and Pfeifer, G. P. (1997) Sequence-specific and domain-specific DNA repair in xeroderma pigmentosum and Cockayne syndrome cells. *J. Biol. Chem. 272*, 20747–20755.
11. Liu, J., Akoulitchev, S., Weber, A., Ge, H., Chuikov, S., Libutti, D., Wang, X. W., Conaway, J. W., Harris, C. C., Conaway, R. C., Reinberg, D., and Levens, D. (2001) Defective interplay of activators and repressors with TFIH in xeroderma pigmentosum. *Cell 104*, 353–363.
12. Oh, K. S., Khan, S. G., Jaspers, N. G., Raams, A., Ueda, T., Lehmann, A., Friedmann, P. S., Emmert, S., Gratchev, A., Lachlan, K., Lucassan, A., Baker, C. C., and Kraemer, K. H. (2006) Phenotypic heterogeneity in the XPB DNA helicase gene (ERCC3): xeroderma pigmentosum without and with Cockayne syndrome. *Hum. Mutat. 27*, 1092–1103.
13. Weeda, G., van Ham, R. C., Vermeulen, W., Bootsma, D., van der Eb, A. J., and Hoeijmakers, J. H. (1990) A presumed DNA helicase encoded by ERCC-3 is involved in the human repair disorders xeroderma pigmentosum and Cockayne's syndrome. *Cell 62*, 777–791.
14. Tirode, F., Busso, D., Coin, F., and Egly, J. M. (1999) Reconstitution of the transcription factor TFIIH: assignment of functions for the three enzymatic subunits, XPB, XPD, and cdk7. *Mol. Cell 3*, 87–95.
15. Douziech, M., Coin, F., Chipoulet, J. M., Arai, Y., Ohkuma, Y., Egly, J. M., and Coulombe, B. (2000) Mechanism of promoter melting by the xeroderma pigmentosum complementation group B helicase of transcription factor IIH revealed by protein-DNA photo-cross-linking. *Mol. Cell. Biol. 20*, 8168–8177.
16. Lin, Y. C., Choi, W. S., and Gralla, J. D. (2005) TFIIH XPB mutants suggest a unified bacterial-like mechanism for promoter opening but not escape. *Nat. Struct. Mol. Biol. 12*, 603–607.
17. Coin, F., Oksenych, V., and Egly, J. M. (2007) Distinct roles for the XPB/p52 and XPD/p44 subcomplexes of TFIIH in damaged DNA opening during nucleotide excision repair. *Mol. Cell 26*, 245–256.
18. Moreland, R. J., Tirode, F., Yan, Q., Conaway, J. W., Egly, J. M., and Conaway, R. C. (1999) A role for the TFIIH XPB DNA helicase in promoter escape by RNA polymerase II. *J. Biol. Chem. 274*, 22127–22130.
19. Bradsher, J., Coin, F., and Egly, J. M. (2000) Distinct roles for the helicases of TFIIH in transcript initiation and promoter escape. *J. Biol. Chem. 275*, 2532–2538.
20. Spangler, L., Wang, X., Conaway, J. W., Conaway, R. C., and Dvir, A. (2001) TFIIH action in transcription initiation and promoter escape requires distinct regions of downstream promoter DNA. *Proc. Natl. Acad. Sci. U.S.A. 98*, 5544–5549.
21. Fukuda, A., Nogi, Y., and Hisatake, K. (2002) The regulatory role for the ERCC3 helicase of general transcription factor TFIIH during promoter escape in transcriptional activation. *Proc. Natl. Acad. Sci. U.S.A. 99*, 1206–1211.
22. Iyer, N., Reagan, M. S., Wu, K. J., Canagarajah, B., and Friedberg, E. C. (1996) Interactions involving the human RNA polymerase II transcription/nucleotide excision repair complex TFIIH, the nucleotide excision repair protein XPG, and Cockayne syndrome group B (CSB) protein. *Biochemistry 35*, 2157–2167.
23. Jawhari, A., Laine, J. P., Dubaele, S., Lamour, V., Poterszman, A., Coin, F., Moras, D., and Egly, J. M. (2002) p52 mediates XPB function within the transcription/repair factor TFIIH. *J. Biol. Chem. 277*, 31761–31767.
24. Weeda, G., Rossignol, M., Fraser, R. A., Winkler, G. S., Vermeulen, W., van't Veer, L. J., Ma, L., Hoeijmakers, J. H., and Egly, J. M. (1997) The XPB subunit of repair/transcription factor TFIIH directly interacts with SUG1, a subunit of the 26S proteasome and putative transcription factor. *Nucleic Acids Res. 25*, 2274–2283.
25. Wang, X. W., Yeh, H., Schaeffer, L., Roy, R., Moncollin, V., Egly, J. M., Wang, Z., Freidberg, E. C., Evans, M. K., Taffe, B. G., et al. (1995) p53 modulation of TFIIH-associated nucleotide excision repair activity. *Nat. Genet. 10*, 188–195.
26. Wang, X. W., Vermeulen, W., Coursen, J. D., Gibson, M., Lupold, S. E., Forrester, K., Xu, G., Elmore, L., Yeh, H., Hoeijmakers, J. H., and Harris, C. C. (1996) The XPB and XPD DNA helicases are components of the p53-mediated apoptosis pathway. *Genes Dev. 10*, 1219–1232.
27. Takeda, N., Shibuya, M., and Maru, Y. (1999) The BCR-ABL oncoprotein potentially interacts with the xeroderma pigmentosum group B protein. *Proc. Natl. Acad. Sci. U.S.A. 96*, 203–207.
28. Maru, Y., Kobayashi, T., Tanaka, K., and Shibuya, M. (1999) BCR binds to the xeroderma pigmentosum group B protein. *Biochem. Biophys. Res. Commun. 260*, 309–312.
29. Maru, Y., Bergmann, E., Coin, F., Egly, J. M., and Shibuya, M. (2001) TFIIH functions are altered by the P210BCR-ABL oncoprotein produced on the Philadelphia chromosome. *Mutat. Res. 483*, 83–88.
30. Nishino, T., Komori, K., Ishino, Y., and Morikawa, K. (2005) Structural and functional analyses of an archaeal XPF/Rad1/Mus81 nuclease: asymmetric DNA binding and cleavage mechanisms. *Structure 13*, 1183–1192.
31. Newman, M., Murray-Rust, J., Lally, J., Rudolf, J., Fadden, A., Knowles, P. P., White, M. F., and McDonald, N. Q. (2005) Structure of an XPF endonuclease with and without DNA suggests a model for substrate recognition. *EMBO J. 24*, 895–905.
32. Roberts, J. A., and White, M. F. (2005) DNA end-directed and processive nuclease activities of the archaeal XPF enzyme. *Nucleic Acids Res. 33*, 6662–6670.
33. Fan, L., Arvai, A. S., Cooper, P. K., Iwai, S., Hanaoka, F., and Tainer, J. A. (2006) Conserved XPB core structure and motifs for DNA unwinding: implications for pathway selection of transcription or excision repair. *Mol. Cell 22*, 27–37.
34. Salerno, V., Napoli, A., White, M. F., Rossi, M., and Ciaramella, M. (2003) Transcriptional response to DNA damage in the archaeon *Sulfolobus solfataricus*. *Nucleic Acids Res. 31*, 6127–6138.
35. Rudolf, J., Makrantoni, V., Ingledew, W. J., Stark, M. J., and White, M. F. (2006) The DNA repair helicases XPD and FancJ have essential iron-sulfur domains. *Mol. Cell 23*, 801–808.
36. Richards, J. D., Cubeddu, L., Roberts, J., Liu, H., and White, M. F. (2008) The archaeal XPB protein is a ssDNA-dependent ATPase with a novel partner. *J. Mol. Biol. 376*, 634–644.
37. Weeda, G., van Ham, R. C., Masurel, R., Westerveld, A., Odijk, H., de Wit, J., Bootsma, D., van der Eb, A. J., and Hoeijmakers, J. H. (1990) Molecular cloning and biological characterization of the human excision repair gene ERCC-3. *Mol. Cell. Biol. 10*, 2570–2581.
38. Hwang, J. R., Moncollin, V., Vermeulen, W., Seroz, T., van Vuuren, H., Hoeijmakers, J. H., and Egly, J. M. (1996) A $3' \rightarrow 5'$ XPB helicase defect in repair/transcription factor TFIIH of xeroderma pigmentosum group B affects both DNA repair and transcription. *J. Biol. Chem. 271*, 15898–15904.
39. Coin, F., Auriol, J., Tapias, A., Clivio, P., Vermeulen, W., and Egly, J. M. (2004) Phosphorylation of XPB helicase regulates TFIIH nucleotide excision repair activity. *EMBO J. 23*, 4835–4846.

40. Sweder, K. S., and Hanawalt, P. C. (1994) The COOH terminus of suppressor of stem loop (SSL2/RAD25) in yeast is essential for overall genomic excision repair and transcription-coupled repair. *J. Biol. Chem. 269*, 1852–1857.
41. Sung, P., Higgins, D., Prakash, L., and Prakash, S. (1988) Mutation of lysine-48 to arginine in the yeast RAD3 protein abolishes its ATPase and DNA helicase activities but not the ability to bind ATP. *EMBO J. 7*, 3263–3269.
42. Sambrook, J., and Russell, D. (2001) *Molecular Cloning: A Laboratory Manual*, 3rd ed., Cold Spring Harbor Laboratory Press, Cold Spring Harbor, NY.
43. Lanzetta, P. A., Alvarez, L. J., Reinach, P. S., and Candia, O. A. (1979) An improved assay for nanomole amounts of inorganic phosphate. *Anal. Biochem. 100*, 95–97.
44. Poterszman, A., Lamour, V., Egly, J. M., Moras, D., Thierry, J. C., and Poch, O. (1997) A eukaryotic XPB/ERCC3-like helicase in *Mycobacterium leprae*? *Trends Biochem. Sci. 22*, 418–419.
45. Altschul, S. F., Gish, W., Miller, W., Myers, E. W., and Lipman, D. J. (1990) Basic local alignment search tool. *J. Mol. Biol. 215*, 403–410.
46. Weeda, G., Eveno, E., Donker, I., Vermeulen, W., Chevallier-Lagente, O., Taieb, A., Stary, A., Hoeijmakers, J. H., Mezzina, M., and Sarasin, A. (1997) A mutation in the XPB/ERCC3 DNA repair transcription gene, associated with trichothiodystrophy. *Am. J. Hum. Genet. 60*, 320–329.
47. Riou, L., Zeng, L., Chevallier-Lagente, O., Stary, A., Nikaido, O., Taieb, A., Weeda, G., Mezzina, M., and Sarasin, A. (1999) The relative expression of mutated XPB genes results in xeroderma pigmentosum/Cockayne's syndrome or trichothiodystrophy cellular phenotypes. *Hum. Mol. Genet. 8*, 1125–1133.
48. Evans, E., Moggs, J. G., Hwang, J. R., Egly, J. M., and Wood, R. D. (1997) Mechanism of open complex and dual incision formation by human nucleotide excision repair factors. *EMBO J. 16*, 6559–6573.
49. Choi, W. S., Lin, Y. C., and Gralla, J. D. (2004) The *Schizosaccharomyces pombe* open promoter bubble: mammalian-like arrangement and properties. *J. Mol. Biol. 340*, 981–989.
50. Ma, L., Siemssen, E. D., Noteborn, H. M., and van der Eb, A. J. (1994) The xeroderma pigmentosum group B protein ERCC3 produced in the baculovirus system exhibits DNA helicase activity. *Nucleic Acids Res. 22*, 4095–4102.
51. Gong, C., Bongiorno, P., Martins, A., Stephanou, N. C., Zhu, H., Shuman, S., and Glickman, M. S. (2005) Mechanism of nonhomologous end-joining in mycobacteria: a low-fidelity repair system driven by Ku, ligase D and ligase C. *Nat. Struct. Mol. Biol. 12*, 304–312.
52. Bagwell, C. E., Bhat, S., Hawkins, G. M., Smith, B. W., Biswas, T., Hoover, T. R., Saunders, E., Han, C. S., Tsodikov, O. V., and Shimkets, L. J. (2008) Survival in nuclear waste, extreme resistance, and potential applications gleaned from the genome sequence of *Kineococcus radiotolerans* SRS30216. *PLoS ONE 3*, e3878.
53. Fall, S., Mercier, A., Bertolla, F., Calteau, A., Gueguen, L., Perriere, G., Vogel, T. M., and Simonet, P. (2007) Horizontal gene transfer regulation in bacteria as a "spandrel" of DNA repair mechanisms. *PLoS ONE 2*, e1055.
54. Lamichhane, G., Zignol, M., Blades, N. J., Geiman, D. E., Dougherty, A., Grosset, J., Broman, K. W., and Bishai, W. R. (2003) A postgenomic method for predicting essential genes at subsaturation levels of mutagenesis: application to *Mycobacterium tuberculosis*. *Proc. Natl. Acad. Sci. U.S.A. 100*, 7213–7218.
55. Maluf, N. K., Fischer, C. J., and Lohman, T. M. (2003) A dimer of *Escherichia coli* UvrD is the active form of the helicase in vitro. *J. Mol. Biol. 325*, 913–935.
56. Kyono, K., Miyashiro, M., and Taguchi, I. (2003) Characterization of ATPase activity of a hepatitis C virus NS3 helicase domain, and analysis involving mercuric reagents. *J. Biochem. (Tokyo) 134*, 505–511.

BI8022416